Plant Physiology, September 1999, Vol. 121, pp. 263–271, www.plantphysiol.org © 1999 American Society of Plant Physiologists

Carbon Metabolism in Spores of the Arbuscular Mycorrhizal Fungus *Glomus intraradices* as Revealed by Nuclear Magnetic Resonance Spectroscopy[1]

Berta Bago, Philip E. Pfeffer*, David D. Douds, Jr., Janine Brouillette, Guillaume Bécard, and Yair Shachar-Hill

United States Department of Agriculture-Agricultural Research Service, Eastern Regional Research Center, 600 East Mermaid Lane, Wyndmoor, Pennsylvania 19038 (B.B., P.E.P., D.D.D., J.B.); Unité Mixte de Recherche, Centre National de la Recherche Scientifique (Strasbourg, France)/Université de Paris-Sud 5546, Pôle de Biotechnologie Végétale, 24 chemin de Borde-Rouge 31326, Castanet Tolosan, France (G.B.); and New Mexico State University, Department of Chemistry and Biochemistry, Las Cruces, New Mexico 88001 (Y.S.-H.)

Arbuscular mycorrhizal (AM) fungi are obligate symbionts that colonize the roots of over 80% of plants in all terrestrial environments. Understanding why AM fungi do not complete their life cycle under free-living conditions has significant implications for the management of one of the world's most important symbioses. We used ^{13}C-labeled substrates and nuclear magnetic resonance spectroscopy to study carbon fluxes during spore germination and the metabolic pathways by which these fluxes occur in the AM fungus *Glomus intraradices*. Our results indicate that during asymbiotic growth: (a) sugars are made from stored lipids; (b) trehalose (but not lipid) is synthesized as well as degraded; (c) glucose and fructose, but not mannitol, can be taken up and utilized; (d) dark fixation of CO_2 is substantial; and (e) arginine and other amino acids are synthesized. The labeling patterns are consistent with significant carbon fluxes through gluconeogenesis, the glyoxylate cycle, the tricarboxylic acid cycle, glycolysis, non-photosynthetic one-carbon metabolism, the pentose phosphate pathway, and most or all of the urea cycle. We also report the presence of an unidentified betaine-like compound. Carbon metabolism during asymbiotic growth has features in between those presented by intraradical and extraradical hyphae in the symbiotic state.

Fossil evidence (Taylor et al., 1995) and molecular phylogenetic studies (Simon et al., 1993) indicate that 400 million years ago the roots of land plants were colonized by ancestors of modern arbuscular mycorrhizal (AM) fungi. Today, more than 80% of land plants still acquire nutrients from soil using arbuscular mycorrhizas, reflecting the evolutionary success of this mutualistic symbiosis (Jakobsen, 1995; Smith and Read, 1997). During arbuscular mycorrhiza formation, plant and fungus integrate structurally and functionally to become a single supraorganism (Azcón-Aguilar and Bago, 1994) whose physiological capacities are superior to those of either organism alone (Jakobsen, 1995). This integration improves nutrient uptake by the plant and allows the heterotrophic, obligately symbiotic fungus to complete its life cycle. Understanding AM physiology has practical and fundamental significance, but requires first a knowledge of the metabolism of each partner.

Carbon metabolism of AM fungi has been reviewed by Jakobsen (1995). Lipids are the major form of carbon in AM fungal spores, hyphae, and vesicles (Cox et al., 1975), comprising 45% to 95% of the spore C pool, depending on the species (Beilby, 1983; Jabaji-Hare, 1988; Bécard et al., 1991). Triacylglycerides account for most of the lipids in spores (Beilby and Kidby, 1980; Jabaji-Hare, 1988; Gaspar et al., 1994). During spore germination (AM fungal asymbiotic growth), the triacylglyceride content remains constant for approximately 5 d (Bécard et al., 1991; Gaspar et al., 1994), after which time it decreases (Beilby and Kidby, 1980; Gaspar et al., 1994), probably through the activity of a membrane-bound lipase (Gaspar et al., 1997). At the same time, an increase in phospholipids is observed during germ tube growth (Beilby and Kidby, 1980). This latter result, together with the incorporation of label from ^{14}C-acetate into triacylglycerides during spore imbibition, led Beilby (1983) to suggest that lipid synthesis and breakdown occurred simultaneously during AM fungal asymbiotic growth.

The dominant storage carbohydrates detected in AM fungal hyphae and spores are glycogen and trehalose (Amijee and Stribley, 1987; Bécard et al., 1991; Bonfante et al., 1994; Shachar-Hill et al., 1995; Bago et al., 1998; Pfeffer et al., 1999). In vivo ^{13}C-NMR studies revealed that such carbohydrates were formed by the AM fungus *Glomus etunicatum* shortly after providing colonized leek roots with ^{13}C-labeled Glc (^{13}C-Glc) (Shachar-Hill et al., 1995). Half of the trehalose stored in *G. etunicatum* spores is broken down during the 5 d after germ tube emergence, indicating that this carbohydrate sustains fungal growth at

[1] This work was supported in part by grant no. 97–35107–4375 from the National Research Initiative Competitive Grants Program/U.S. Department of Agriculture and via a fellowship under the Organisation for Economic Co-operation and Development Co-operative Research Program: Biological Resource Management for Sustainable Agriculture Systems (to G.B.). The research utilized in part the Resource for Solid-State NMR of Proteins at the University of Pennsylvania: A National Institutes of Health Supported Research Center (grant no. P41RR09731 from the Biomedical Research Technology Program, National Center for Research Resources, National Institutes of Health).

* Corresponding author; e-mail ppfeffer@arserrc.gov; fax 215–233–6581.

the very early stages of germination (and prior to lipid breakdown) (Bécard et al., 1991). CO_2 also seems to play an important role in AM fungal axenic growth: Bécard and Piché (1989) found a 10-fold increase in *Gigaspora margarita* germ tube development when a 0.5% CO_2 atmosphere was supplied.

Assays of enzymatic activities have indicated the presence of several metabolic pathways during asymbiotic growth of *Glomus mosseae* (Macdonald and Lewis, 1978) and *Gi. margarita* (Saito, 1995). Of the glycolytic enzymes, phosphofructokinase (EC 2.7.1.11) and glyceraldehyde-P dehydrogenase (EC 1.2.1.12) have been detected (Macdonald and Lewis, 1978; Saito, 1995). The presence of the tricarboxylic acid cycle (TCA) enzymes malate dehydrogenase (EC 1.1.1.37) and succinate dehydrogenase (EC 1.3.5.1) has also been demonstrated (Macdonald and Lewis, 1978; Saito, 1995). The activity of Glc-6-P dehydrogenase (EC 1.1.1.49) (Macdonald and Lewis, 1978; Saito, 1995) was found to be higher in germinated spores of *Gi. margarita* than in intraradical hyphae (Saito, 1995), suggesting a role for the pentose phosphate pathway (PPP) in the developing spore. More recently, the presence of the enzyme 3-phosphoglycerate kinase (EC 2.7.2.3) has been revealed by differential RNA display in *G. mosseae* germinating spores and mycorrhizal roots (Harrier et al., 1998). This enzyme is implicated in both glycolysis and gluconeogenesis.

Recently, Pfeffer et al. (1999) used AM monoxenic cultures of *Glomus intraradices* and Ri T-DNA-transformed carrot (*Daucus carota*) roots to study C metabolism in the symbiotic state. That study indicated that uptake, transport, and metabolism are very different in the intraradical and extraradical parts of AM fungi in the symbiotic state. Whereas intraradical fungal structures take up carbon (as hexose) and synthesize lipids, the extraradical mycelium does neither. Since earlier results indicated differences in the metabolism of the AM fungus when growing in symbiosis or asymbiotically (Harrison and van Buuren, 1995; Shachar-Hill et al., 1995), the aim of the present work was to extend our knowledge of the sources and fates of C compounds during AM fungal spore germination and the metabolic pathways connecting both.

MATERIALS AND METHODS

Production and Labeling of Spores

Ri T-DNA-transformed carrot (*Daucus carota* L.) roots colonized by *Glomus intraradices* Schenck & Smith (DAOM 197198, Biosystematic Research Center, Ottawa) were grown in Petri plates with two compartments as described by St-Arnaud et al. (1996). The roots were confined to one compartment but the fungus was allowed to grow over the divider and into the other compartment. In the following 9 to 10 weeks the fungus grew and sporulated extensively in this fungal compartment. To produce prelabeled spores, $^{13}C_1$-Glc was added to the medium through a sterile filter (25 mM final concentration) in the compartment containing the mycorrhizal roots 1 to 2 weeks after the fungus had crossed the plastic barrier (Pfeffer et al., 1999).

Spores and extraradical hyphae from the fungal compartment were recovered by blending the solidified medium in sodium citrate solution (10 mM) at high speed for 45 s in a commercial blender (Waring). Fungal tissue was collected on a 38-μm sieve and rinsed with water. Spores from the fungal compartments of three plates were combined for each sample. For ungerminated spore samples, fungal tissue was frozen at −80°C immediately after collection. Spores were germinated while incubating in liquid M medium (Bécard and Fortin, 1988) without Suc for 14 d (32°C in 2% CO_2, in the dark). When prelabeled spores were germinated, no carbon source was added to the liquid medium. ^{13}C-labeled substrates (99% ^{13}C-enriched) were added as filter-sterilized solutions to the M medium of unlabeled spores for a final concentration of 25 mM for $^{13}C_1$- or $^{13}C_{1,2}$-Glc, $^{13}C_1$-Fru, or $^{13}C_1$-mannitol experiments and to 4 mM for $^{13}C_1$- or $^{13}C_2$-acetate experiments. For $^{13}CO_2$ labeling, unlabeled spores were incubated at room temperature in the presence of 2% $^{13}CO_2$ (generated by addition of a 50% solution of lactic acid to solid $K_2{}^{13}CO_3$ in a sealed 6-L desiccator). In all cases more than 80% of the spores germinated within 3 d and formed a macroscopically visible diffuse mycelium during the incubation period. After incubation, the fungal material was recovered and frozen at −80°C until carbohydrate and lipid extraction.

Extraction and NMR Sample Preparation

Extracts were prepared as previously described (Pfeffer et al., 1999) with minor modifications. Samples were lyophilized and ground with a mortar and pestle with acid-washed sand at −20°C in 40 mL of methanol:water (MeOH:H_2O) (70:30, v/v). After filtration using Whatman no. 2 filter paper, the methanol was removed by evaporation under reduced pressure and the aqueous solution was freeze-dried. For NMR analysis, the extract was dissolved in 750 μL of ^{2}H water and insoluble matter was removed by centrifugation.

To extract neutral lipids and fatty acids, the solid residue remaining after MeOH/H_2O extraction was freeze-dried and re-extracted in 30 to 40 mL of boiling isopropyl alcohol for 20 min. After filtering, the solvent was removed by evaporation under a stream of nitrogen. These extracts were dissolved in ^{2}H chloroform for NMR analysis.

NMR Spectroscopy

Spectra were obtained using a 400 MHz spectrometer (UnityPlus, Varian, Palo Alto, CA) with a superconducting magnet (9.4T, Oxford Instruments, Concord, MA), although several ^{1}H extract spectra were acquired at 600 and 750 MHz on spectrometers (Brüker, Billerica, MA). A 5-mm broad-band probe was used for ^{13}C spectra, while a 5-mm, ^{1}H inverse-detection probe with a Z gradient and broad-band decoupling coils was used for ^{1}H and ^{1}H-^{13}C correlation spectra.

^{13}C spectra were accumulated with 80° pulse angles, WALTZ-^{1}H decoupling, and a recycle time of 4.2 s (MeOH extracts) or 13.2 s (isopropyl alcohol extracts). For ^{1}H spectra, 80° pulses and recycle times of 4.5 s were used; when

necessary, 12-s recycle times were employed to prevent distortion of the relative intensities of the ^{1}H-^{12}C and ^{1}H-^{13}C signals (London, 1988). Total acquisition times for both ^{13}C and ^{1}H extracts were between 12 and 36 h depending on the concentration of each sample.

The identification of peaks in ^{13}C and ^{1}H spectra was made from literature values (Gunstone et al., 1977, for lipids; Fan, 1995, for all other metabolite assignments), via comparison of spectra of purified compounds (e.g. trehalose in Fig. 1A) or natural abundance (n.a.) signals of unlabeled tissue extracts (e.g. Fig. 1B), by spiking extracts with purified compounds, and/or by analyses of ^{1}H and ^{1}H-^{13}C correlation spectra (Pfeffer et al., 1999). ^{13}C chemical shifts were referenced to the signals of C_1-trehalose (T_1, 94.1 ppm) or chloroform (77.0 ppm). ^{1}H signals were referenced to water (4.67 ppm at 35°C) or to the chloroform peak (7.24 ppm). Carbon and proton shifts were expressed in parts per million with respect to tetramethylsilane at 0 ppm.

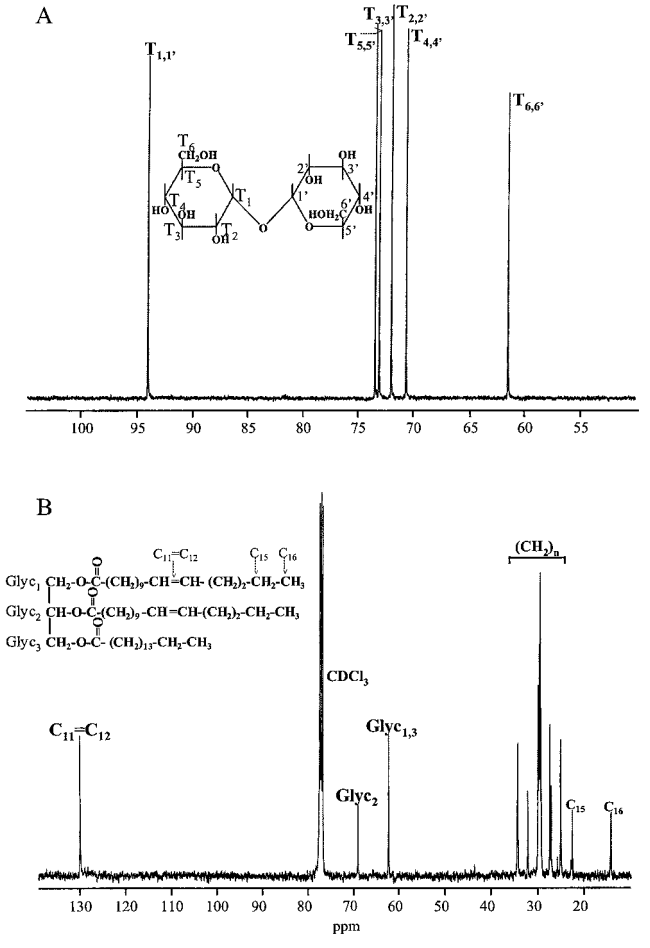

Figure 1. ^{13}C-n.a. signals of trehalose (A) and an isopropyl alcohol extract of unlabeled AM fungal spores (B). Insets, Chemical structure of trehalose and of a triacylglyceride showing the correspondence between the different C positions and their chemical shift in the NMR spectra.

Quantification of ^{13}C-Labeling

^{13}C-Isotopic abundance (atom percent ^{13}C) of the labeled positions of a given compound was calculated by comparison with n.a. ^{13}C-isotopic signals of unlabeled positions of the same compound and/or by measurement of the ^{13}C-^{1}H satellites of ^{1}H signals in proton spectra. Specifically, the satellites of the ^{1}H signals coupled to carbons: (a) 1,1′ of trehalose at 5.18 ppm (Fig. 2C, inset); (b) of the unknown betaine at 3.25 ppm (Fig. 2A, inset) for MeOH/H_2O extracts; (c) of the methyl group (C_{16}) of fatty acids at 0.88 ppm (not shown); and (d) at the 1 and 3 positions of glyceryl (Gly_1, Gly_3) (4.2 ppm) for lipid extracts (Fig. 3A, inset) were routinely used. From these measures of absolute ^{13}C content, the ^{13}C content at other positions was then deduced by comparison of the intensities of the respective resonances in the ^{13}C spectra.

RESULTS

Labeling in Fungal Carbohydrate

Representative ^{13}C-NMR spectra obtained for the MeOH/H_2O extracts from each treatment are shown in Figure 2. Peaks at 94.1, 73.4, 72.9, 71.9, 70.5, and 61.4 ppm correspond to the chemical shifts of carbons (1,1′), (3,3′), (5,5′), (2,2′), (4,4′), and (6,6′) of trehalose (Fig. 2, T_1–T_6, compare with Fig. 1A). The predominance of trehalose signals in such spectra is in accordance with previous studies (Bécard et al., 1991, Pfeffer et al., 1999) in which trehalose was the most abundant extracted carbohydrate in AM fungal spores.

Levels of ^{13}C-labeling (percent in excess of n.a.) for each C position of fungal trehalose (T_1–T_6) following various labeling treatments are shown in Table I. In prelabeled, non-germinated spores (Fig. 2A), labeling was found in all C positions, with T_1, T_6, T_5, and T_3 having the most incorporation of label. When ^{13}C-prelabeled spores were germinated without exogenous label, a similar pattern was observed in trehalose with slight decreases in T_1 and T_3 labeling (Fig. 2B; Table I).

Spores germinated for 14 d showed different ^{13}C-labeling patterns depending on the substrate provided. Spores exposed to $^{13}C_1$-Glc (Fig. 2C) or $^{13}C_1$-Fru (not shown) yielded trehalose mostly labeled in T_1 (Table I). We observed no evidence of scrambling of the label provided as T_1 into the T_6 position. These results were confirmed when using $^{13}C_{1,2}$-Glc as a substrate (Table I), with most of the label being found in the T_1 and T_2 positions. Incubation with $^{13}C_{1,6}$-mannitol produced no labeling in trehalose or elsewhere (not shown). Spore germination in the presence of either $^{13}CO_2$ or $^{13}C_1$-acetate yielded trehalose with the highest labeling found in the T_4 position (Fig. 2, D and E; Table I). In these two treatments the T_3 position was also highly labeled, T_2 and T_1 were less so, and T_6 and T_5 were either minimally labeled or unlabeled. In contrast, upon exposure to $^{13}C_2$-acetate, detected fungal trehalose displayed a very different labeling pattern, with T_4 containing the least amount of label and T_6 and T_5 having the highest (Fig. 2F; Table I). This latter labeling pattern closely resem-

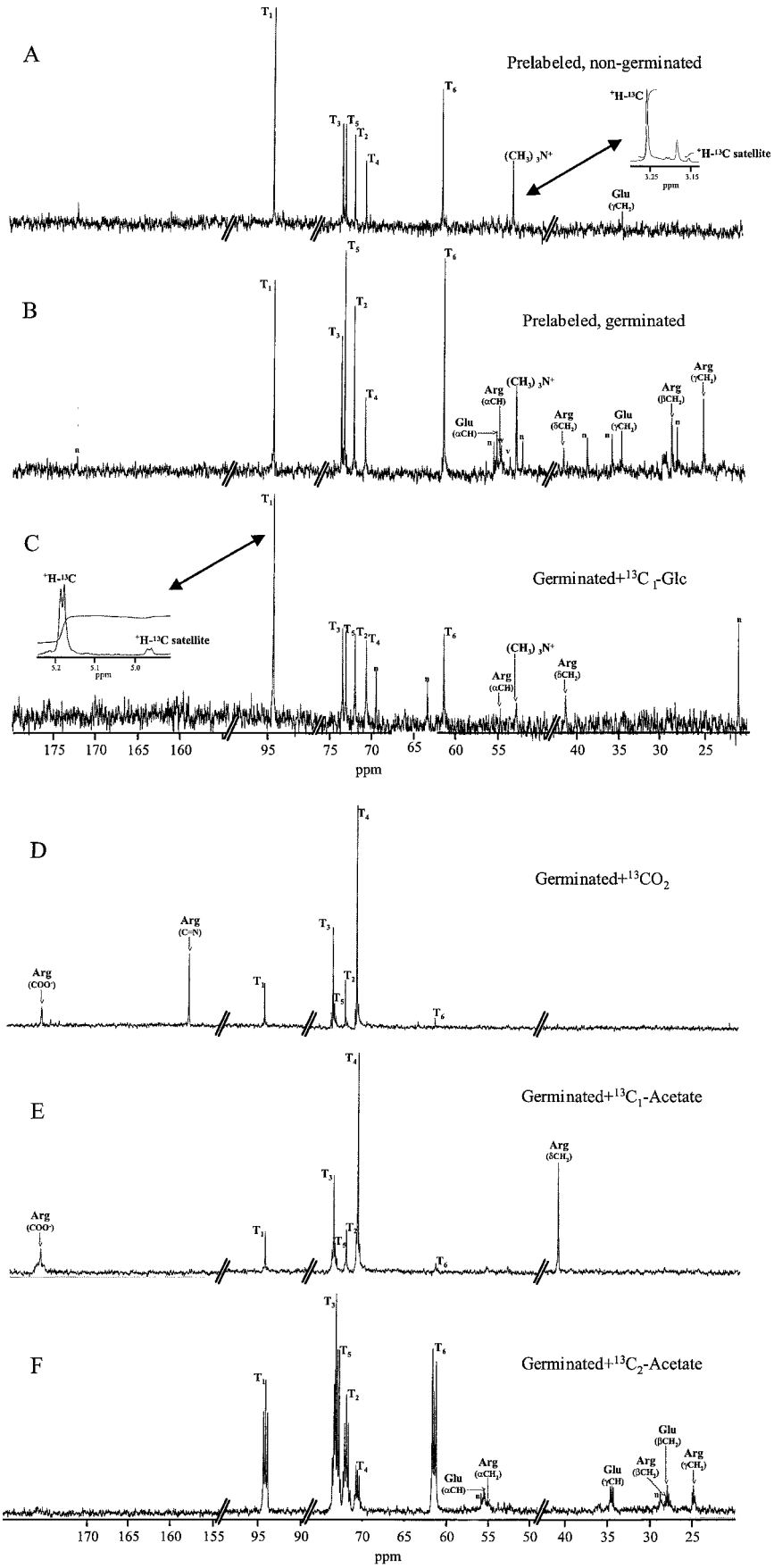

Figure 2. ^{13}C-NMR spectra of MeOH/H_2O extracts of asymbiotic fungal tissue following different treatments. A, Spores prelabeled but not germinated. Inset, ^{1}H spectrum of the same sample showing the ^{1}H resonance of the unidentified betaine-like compound and the upfield ^{13}C-^{1}H satellite used for measuring the ^{13}C content in this compound. B, Asymbiotic tissue prelabeled as in A and then germinated for 14 d without external label. C, Unlabeled spores germinated for 14 d in the presence of 25 mM $^{13}C_1$-Glc. Inset, ^{1}H spectrum of the same sample showing the ^{1}H resonance of trehalose and a ^{13}C-^{1}H satellite used for measuring the ^{13}C content in the C_1 position. D, Unlabeled spores germinated for 14 d in the presence of $^{13}CO_2$. E, Same as D, except germinated in the presence of 4 mM $^{13}C_1$-acetate. F, Same as E, except $^{13}C_2$-acetate. T_1 to T_6, Trehalose resonances (C_1–C_6); w, choline; v, GAB-betaine; *n*, unidentified signal.

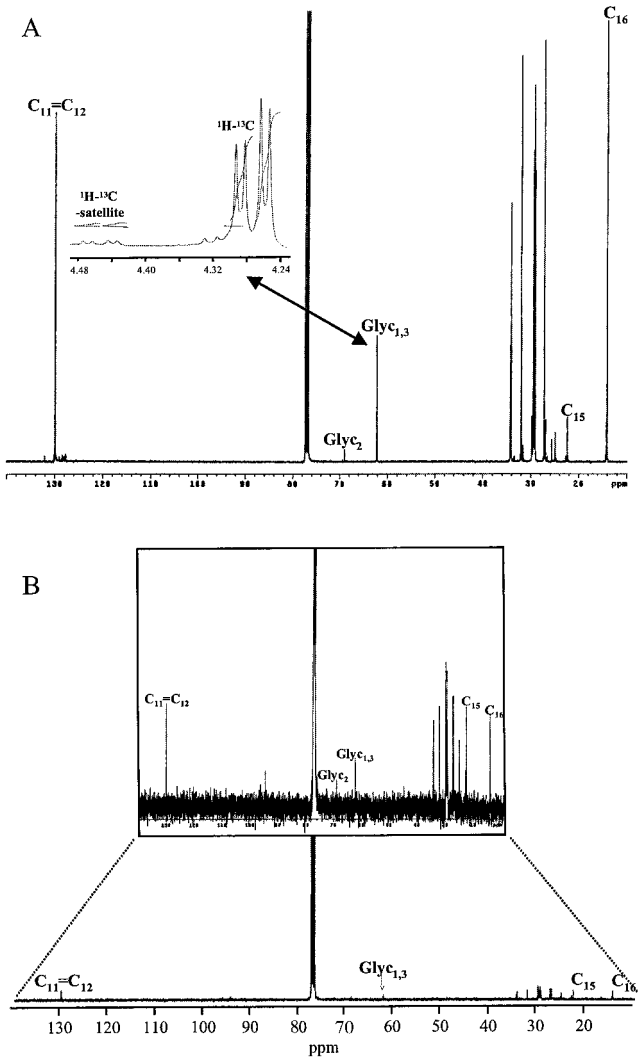

Figure 3. ^{13}C-NMR spectra of isopropyl alcohol extracts. A, Spores prelabeled with $^{13}C_1$-Glc and germinated for 14 d in liquid M medium with no carbon. Inset, ^1H spectrum of the same sample showing the ^1H resonance of the $^{13}Glyc_{1,3}$ and the downfield ^{13}C-^1H satellite used for measuring its ^{13}C content. B, Unlabeled spores germinated for 14 d in M minus C liquid medium in the presence of $^{13}C_1$-Glc. Boxed inset, Spectrum expanded to better detect the signals of interest.

bles the one observed for prelabeled, germinated spores (Table I).

Splittings (multiplets) observed in trehalose peaks, particularly for experiments with $^{13}C_2$-acetate (Fig. 2F) but also in extracts of $^{13}C_1$-acetate and $^{13}CO_2$ labeled samples (Fig. 2, D and E), were due to homonuclear coupling between ^{13}C nuclei at adjacent carbon positions of the same molecules. These couplings arising from multiply-labeled molecules are expected when a product such as hexose is made from more than one molecule of labeled substrate.

The ^{13}C spectra of MeOH/H_2O extracts also showed evidence of labeling in two amino acids: Glu and Arg. The small signals from Glu (Fig. 2, A, B, and F) showed that it was labeled in γ and α carbons in prelabeled, germinated spores, whereas labeling was only detected in the γ carbon in prelabeled, nongerminated spores. Spores germinated in $^{13}C_1$-acetate had labeling in the δCO position (182.0 ppm, not shown), and the ones germinated in $^{13}C_2$-acetate had labeling in the α, γ, and β positions of Glu. The ^{13}C spectra also showed consistent labeling of Arg. Spectra from prelabeled, germinated spores showed labeling at the γ, β, δ, and α carbons of Arg; unlabeled spores germinated in the presence of $^{13}C_1$-Glc showed labeling at the δ and α carbons; $^{13}CO_2$ resulted in labeling in the terminal C═N and carboxyl positions; $^{13}C_1$-acetate labeled δCH_2 and carboxyl groups; and $^{13}C_2$-acetate labeled the γ, α, and β carbons (Fig. 2; Table I). Notably, no Arg signals were found in spectra of prelabeled, non-germinated spores.

A single resonance with a chemical shift of 52.9 ppm in the ^{13}C spectra of MeOH/H_2O extracts of prelabeled spores (germinated or not) arises from an unknown compound (Fig. 2, A and B, $[CH_3]_3N^+$). This ^{13}C signal was shown (by ^1H and ^1H-^{13}C correlation spectra, see "Materials and Methods") to arise from a carbon with attached protons whose signal in the ^1H spectrum is a singlet at 3.25 ppm (Fig. 2A, inset). The ^{13}C and ^1H-chemical shifts and ^{13}C-^1H-coupling (145 Hz) are similar to those of methyl groups of betaines ($[CH_3]_3N^+$). Signals from this putative $(CH_3)_3N^+$ group were also detectable in spectra of unlabeled spores germinated in $^{13}C_1$-Glc (Fig. 2C) and $^{13}C_{1,2}$-Glc (not shown). Estimations of the ^{13}C content of this group (Table I) were carried out by ^1H-^{13}C-satellite measurements (Fig. 2A, inset). The $(CH_3)_3N^+$ peak of this betaine-like compound showed approximately 8% ^{13}C enrichment in prelabeled spores (either germinated or not), but less than 2% in $^{13}C_1$-Glc labeling experiments, whereas in other treatments the $(CH_3)_3N^+$ peak corresponded to n.a. signals.

Labeling in Fungal Lipids

A previous study of this system (Pfeffer et al., 1999) showed that when labeled hexose was provided to the host roots during spore formation (corresponding to the prelabeled, nongerminated spores in this study) fungal lipids became labeled both in glyceryl and fatty acid moieties. Here we observed similar lipid labeling (approximately 8% over n.a.) in prelabeled spores, whether germinated or not (Fig. 3A, $Glyc_{1,3}$:$Glyc_2$ ratio > 2:1; C_{16}:C_{15} ratio > 1:1). However, only n.a. ^{13}C signals were observed in lipids when any of the labeled substrates was supplied to germinating spores (Fig. 3B, $Glyc_{1,3}$:$Glyc_2$ ratio = 2:1; C_{16}:C_{15} ratio = 1:1).

DISCUSSION

The fact that AM fungi do not grow axenically has puzzled and frustrated researchers for over three decades. Limitations in the metabolism or uptake of carbon in the asymbiotic state have been proposed to explain this failure (for review, see Azcón-Aguilar et al., 1998). To test this possibility it is necessary to define which pathways, if any, may be deficient in the germinating spore. To this end, we have compared the labeling patterns in different products

Table I. *^{13}C-Labeling quantification (% over n.a.) of fungal trehalose, Glu, Arg, and the unknown betaine compound ($(CH_3)_3N^+$) in the different treatments assayed*

	Trehalose										(a) Glu (b) Arg	$(CH_3)_3N^+$
Prelabeled, non-germinated	**T_1**	≥	**T_6**	>	**T_5**	~	**T_3**	≥	**T_2**	>	**T_4**	(a) γCH_2 (b) n.d.[a]	8.4
	10.7		9.9		7.5		7.1		5.9		2.6		
	(1.1)[b]		(0.6)		(0.9)		(0.6)		(1.2)		(0.8)		(1.2)
Prelabeled, germinated	**T_6**	≥	**T_1**	~	**T_5**	≥	**T_2**	≥	**T_3**	>	**T_4**	(a) γCH_2, αCH (b)γCH_2, βCH_2, δCH_2, αCH	7.1
	6.3		5.4		5.3		4.4		2.9		1.1		
	(1.8)		(2.2)		(1.4)		(1.9)		(0.4)		(0.2)		(1.8)
Germinated + $^{13}C_1$-Glu	**T_1**	>	**T_3**	~	**T_6**	~	**T_5**	~	**T_2**	~	**T_4**	(a) n.d. (b) δCH_2	++[d]
	5.3		1.0		0.9		n.a.[c]		n.a.		n.a.		
	(2.7)		(0.9)		(0.8)		—		—		—		
Germinated + $^{13}C_{1,2}$-Glu	**T_2**	>	**T_1**	>	**T_3**	~	**T_6**	~	**T_5**	~	**T_4**	(a) n.d. (b) δCH_2	++
	4.7		3.0		0.6		n.a.		n.a.		n.a.		
	(0.9)		(0.1)		(0.1)		—		—		—		
Germinated + $^{13}CO_2$	**T_4**	>	**T_3**	>	**T_1**	≥	**T_2**	>	**T_6**	=	**T_5**	(a) COO (b) C=N>COO	n.a.
	24.4		14.4		5.0		3.8		n.a.		n.a.		
	(2.7)		(0.9)		(0.8)		(0.7)		—		—		
Germinated + $^{13}C_1$-Acetate	**T_4**	>	**T_3**	≥	**T_2**	≥	**T_1**	≥	**T_6**	>	**T_5**	(a) δCOO (b) δCH_2>COO	n.a.
	31.9		15.3		7.3		5.9		5.0		n.a.		
	(11.1)		(5.3)		(3.3)		(1.9)		(0.9)		—		
Germinated + $^{13}C_2$-Acetate	**T_6**	≥	**T_5**	≥	**T_1**	>	**T_3**	≥	**T_2**	>	**T_4**	(a) γCH_2, αCH, βCH_2 (b) γCH_2, βCH_2, αCH	n.a.
	79.1		72.9		60.5		43.9		41.9		18.8		
	(5.2)		(5.9)		(7.3)		(6.6)		(3.9)		(1.6)		

[a] n.d., Not detected. [b] Figures in parentheses express the SD. [c] n.a., ^{13}C-Natural abundance (1.1%). [d] Traces (<2%) of labeling were found.

of metabolism with the patterns expected from the operation of known metabolic pathways. Figure 4 summarizes our interpretation of the results by showing the flow of labeled C from each substrate provided to each product detected via key intermediate compounds whose presence is implied but which were not detected.

Trehalose as an Indicator of Hexose Metabolism

Trehalose became labeled when any of several labeled exogenous precursors was provided to the asymbiotic fungus, demonstrating that it is synthesized during spore germination (Fig. 4, pathway 1). Since trehalose is a Glc dimer, its labeling pattern reflects labeling in hexose within the fungus and therefore can be used to follow hexose uptake and/or synthesis. Previous studies have demonstrated that trehalose levels decrease during spore germination in many fungal species (Thevelein et al., 1982, and refs. therein), among them AM fungi (Bécard et al., 1991) (Fig. 4, pathway 2). Thus, the labeling obtained reflects turnover rather than net production of trehalose (Fig. 4, pathways 1 and 2). This is consistent with observations of rapid synthesis and degradation of trehalose in the symbiotic state (Shachar-Hill et al., 1995) and with the hypothesis by Pfeffer et al. (1999) that trehalose may act to buffer intracellular Glc levels.

Hexose Uptake and Utilization

When germinating spores were exposed to hexose ($^{13}C_1$ or $^{13}C_{1,2}$-Glc, or $^{13}C_1$-Fru) the labeling was observed in trehalose, Glu, Arg, and in an unidentified betaine-like compound (see below). Thus, hexose can enter and be metabolized in the asymbiotic state via glycolysis (pathway 5 of Fig. 4). There was little or no scrambling from the labeled C position(s) of the hexose substrates tested to other positions of trehalose (Table I), suggesting that hexose is directly incorporated into trehalose (Fig. 4, pathway 1). The levels of labeling in trehalose when ^{13}C-hexose was supplied (5%, Table I) were modest compared with other substrates, indicating that in the germinating spore intracellular hexose reaches only a low fractional enrichment. This may be because its uptake is much less than in the intraradical phase (where it reaches 80% within 24 h, Shachar-Hill, 1995) and/or because it is diluted by unlabeled hexose being synthesized internally from other C sources.

Dark Fixation of $^{13}CO_2$ and Gluconeogenesis

The observation of substantial labeling in trehalose when $^{13}CO_2$ is supplied (Table I) demonstrates a significant rate of dark fixation (presumably by pyruvate carboxylase, Fig. 4, pathway 8a). Moreover, the labeling of mainly T_4 and T_3 of trehalose is the pattern usually observed in hexose when labeled CO_2 is supplied to tissues undergoing gluconeogenesis (Fig. 4, pathways 8a, then 8b and 8c, and then 4; see e.g. Brosnan, 1982). Bécard and Piché (1989) showed that CO_2 stimulates the asymbiotic growth of another AM fungus, *Gi. margarita*, and suggested that CO_2 may be a net source of carbon for anabolic processes. Dark fixation as part of gluconeogenesis does not lead to a net gain of C, since the same amount of CO_2 is released by decarboxylation (by PEP carboxykinase to produce PEP, Fig. 4, path-

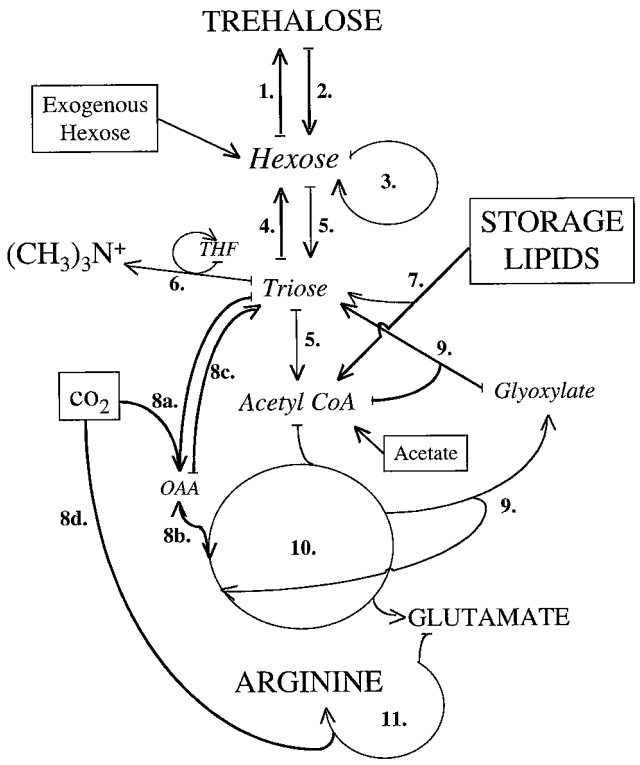

Figure 4. A simplified scheme of the AM fungal metabolic pathways revealed active in the present study. Labeled substrates provided in different experiments are shown in boxes, products detected are shown in capital letters, and certain metabolic intermediates or pools whose presence is inferred but were not detected are shown in italics. 1, Trehalose synthesis from Glc phosphate and UDP-Glc; 2, trehalose breakdown by trehalase; 3, the PPP (also known as the hexose monophosphate pathway); 4, gluconeogenesis, starting with PEP and involving reversal of glycolysis with several differences; 5, glycolysis (the Embden-Meyerhoff-Parnas pathway); 6, non-photosynthetic one-carbon metabolism, typically involving tetrahydrofolate (THF) and *S*-adenosyl Met as carriers of the methyl groups; 7, lipolysis: storage lipid (tryacylglycerides) breakdown to glycerol and fatty acids, and subsequent glyoxysomal fatty acid β-oxidation to acetyl CoA; 8, Dark fixation of CO_2 by pyruvate carboxylase to oxalocetate (8a) or carbamoyl P synthethase (8d); 9, glyoxylate cycle (or shunt) involving the production of glyoxylate from acetyl-CoA units via part of the TCA cycle; the glyoxylate is condensed with acetyl-CoA (from triacylglyceride degradation) to form triose and CO_2; 10, TCA (also known as the Krebs cycle); 11, Arg synthesis by enzymes of the urea cycle including the incorporation of carbon from carbamoyl P.

way 8c) as is fixed by pyruvate carboxylase. However, labeling in the carboxyl of Arg indicates that CO_2 fixation also has an anaplerotic role.

Glyoxylate Cycle

During spore germination, the synthesis of cell walls and DNA, among other anabolic processes, must create large demands for carbohydrate units. Since the majority of carbon storage in AM fungal spores is as lipid and not as carbohydrate, one would expect the conversion of lipids to hexose to be important at this stage of the fungal life cycle. Acetate was used to test this hypothesis, since it is a precursor of acetyl CoA, itself a key intermediate in fatty acid breakdown.

The labeling pattern of trehalose extracted from germinating spores incubated with $^{13}C_1$-acetate was similar to that observed in $^{13}CO_2$ labeling experiments (Table I). This could arise from the liberation (as $^{13}CO_2$) of the labeled C_1 carbon of acetate via the TCA cycle (pathway 10 of Fig. 4) followed by dark re-fixation of the released $^{13}CO_2$, as indicated above. However, the same labeling pattern is also predicted by the conversion of acetate to triose via the glyoxylate cycle (Fig. 4, pathways 9, 4, and 1).

The results of labeling with $^{13}C_2$-acetate suggest that both of these mechanisms occur. The glyoxylate cycle transfers label supplied in C_2 of acetate to carbons 6, 1, 5, and 2 of trehalose (following pathways 9, 4, and 1 of Fig. 4), and the labeling observed in carbons 3 and 4 can be accounted for by release of label as $^{13}CO_2$ (via second and further turns of the TCA cycle) and its refixation (Fig. 4, pathways 8a, 8b, 8c, 4, and 1). The very high level of labeling reached in trehalose when $^{13}C_2$-acetate was provided (close to 80% in T_6) indicates a high metabolic flux from acetyl-CoA to hexose. Such a high flux would be expected if most of the intracellular hexose during the asymbiotic phase were made from storage lipids (sequentially following pathways 7, part of 10, 9, and 4 of Fig. 4).

Results from prelabeled spores are also consistent with conversion of lipid to trehalose during spore germination. The fatty acids in prelabeled spores are labeled predominantly in the even-carbon positions of the fatty acid chains (Pfeffer et al., 1999) and thus yield C_2-labeled acetyl CoA, as would be expected of $^{13}C_2$ acetate. Indeed, the relative enrichment in different positions of the trehalose from prelabeled, germinated spores (Table I) is similar to that after $^{13}C_2$-acetate labeling.

PPP

Gluconeogenic flux from labeled triose to hexose during germination is expected to result in equal labeling in carbons 6 and 1, in carbons 5 and 2, and in 4 and 3. However, we observed markedly asymmetrical trehalose labeling patterns in experiments using both $^{13}C_1$ and $^{13}C_2$-acetate and $^{13}CO_2$ (Table I). Deviation from this symmetrical labeling pattern can arise in hexose due to the action of the PPP (Fig. 4, pathway 3). The scrambling expected from the operation of the PPP can explain the patterns of asymmetry observed in trehalose: $C_4 > C_3$ from $^{13}C_1$-acetate and from $^{13}CO_2$, but $C_3 > C_4$ from $^{13}C_2$-acetate. The operation of the PPP is also consistent with the labeling of C_1 and C_2, and the absence of labeling in C_5 and C_6 of trehalose when $^{13}CO_2$ or $^{13}C_1$-acetate were provided. The PPP is known to be active in fungi (for review, see Jennings, 1995) and its action is consistent with recent observations in the symbiotic state (Pfeffer et al., 1999). However, the results of labeling with $^{13}C_{1,2}$-Glc (Table I) do not indicate any PPP activity, since in this case the PPP should result in greater labeling in C_1 than in C_2. Moreover, estimations of PPP activity carried out in this study (by comparing the central peak of the labeled positions T_1 or T_2 with the single peak

of the n.a. positions T_6, T_5, or T_4 when $^{13}C_{1,2}$-Glc was provided exogenously) resulted in no apparent activity of this metabolic pathway. Further experiments are required before alternative explanations (such as more than one intracellular hexose pool) can be fruitfully proposed.

Amino Acid Synthesis

^{13}C-Labeling of Glu and Arg shows that these amino acids are synthesized during asymbiotic fungal growth. Whereas Glu labeling was also detected during the symbiotic phase (seen in prelabeled, non-germinated spores), Arg synthesis was only detected during germination (Table I). The patterns of labeling in both amino acids from the various labeled substrates are consistent with the usual biosynthetic routes (Fig. 4, pathways 5 and 10 for Glu; pathways 5, 10, 8d, and 11 for Arg). The production and labeling of Arg reveals the presence and operation in the asymbiotic AM fungus of most enzymes of the urea cycle (Fig. 4, pathway 11), although there is no evidence that the last step, which produces urea (through arginase activity), is active.

There are a number of possible roles for Arg during AM fungal spore germination. One of them is as a charge balance for polyphosphates (Cramer et al., 1980; Cramer and Davis, 1984; Bücking et al., 1998). However, the state of polyphosphates in mycorrhizal fungi has been the subject of considerable debate (Kulaev, 1979; Martin et al., 1985; Orlovich and Ashford, 1993; Bücking et al., 1998), and in our view, there is still no conclusive evidence that Arg (or other basic amino acids in the fungal vacuole) is bound to these macromolecules. Other possible explanations for the observed formation of Arg during germination include roles in nitrogen storage, as a compatible osmolyte, and as a possible form of N transferred to the host.

A Betaine-Like Compound

We consistently observed in the spectra of prelabeled spores (either germinated or not) and of spores germinated in the presence of ^{13}C-Glc, ^{1}H and ^{13}C signals from an unidentified compound. Because of a number of spectroscopic characteristics we believe that these signals arose from the nitrogen-bonded methyl groups of a betaine-like molecule. The reasons for this tentative assignment include: (a) the spectral position of the ^{1}H and ^{13}C signals compared with known betaines, (b) the absence of homonuclear couplings in the ^{1}H signal, (c) the size of the coupling constant between ^{1}H and ^{13}C, and (d) the liberation of trimethylamine upon heating (not shown). The fact that labeling of this compound was not observed in ^{13}C-acetate-labeling experiments indicates that it is not made from lipids. The labeling obtained when $^{13}C_1$-Glc was used is consistent with the origin of methyl groups through non-photosynthetic one-carbon metabolism from hexose via Ser (Fig. 4, pathways 5 and 6).

Absence of Storage Lipid Synthesis

None of the substrates provided during spore germination resulted in detectable labeling of lipids. Since there is clear evidence that acetyl-CoA becomes significantly labeled by at least ^{13}C-acetate, we would expect to detect labeling if 1% or more of the lipid had been synthesized during the incubation period. We therefore believe that, in contrast to trehalose, storage lipids are not synthesized to any great extent during asymbiotic fungal growth. Beilby (1983) found modest labeling of triacylglycerides when ^{14}C-acetate was provided to *G. caledonium* spores during spore imbibition. This difference may reflect the much greater sensitivity of radiotracer methods or the different timing of the experiments. Beilby's data also showed a consistent increase in the labeling of the phospholipid fraction during germination, which is indicative of membrane synthesis. Since our isopropyl alcohol extracts contained predominantly neutral storage lipids (Pfeffer et al., 1999), we believe that during germination, lipid synthesis is largely or entirely confined to membrane production.

Carbon Metabolism in the Asymbiotic versus the Symbiotic AM Fungus

Previous studies have shown that during symbiosis, intraradical and extraradical parts of AM fungi are very different in their C metabolism: substantial hexose uptake occurs in the intraradical phase (Shachar-Hill et al., 1995; Saito, 1995, Solaiman and Saito, 1997; Pfeffer et al., 1999) and here also is the site of storage lipid synthesis. In contrast, extraradical hyphae are unable to take up hexose and do not synthesize storage lipids (these are transported from the intraradical to the extraradical mycelium, Pfeffer et al., 1999). When growing asymbiotically, AM fungi have characteristics in common with each of the two metabolic states described above. That is, both hexose and acetate can enter the AM germ tubes and be metabolized; however, the synthesis of storage lipids is either blocked or greatly reduced in the asymbiotic fungus. Since gluconeogenesis and the glyoxylate cycle involving lipid breakdown are active pathways in asymbiotic germ tubes, it may be that a transition from catabolism to anabolism of lipids (initiated when intimate contact is established with the host plant) is essential to the AM fungus in order to fully develop and complete its life cycle.

ACKNOWLEDGMENT

We thank Dr. Kathleen Valentine of the University of Pennsylvania NMR facility for obtaining some of the ^{13}C-^{1}H satellite spectra.

Received March 24, 1999; accepted June 9, 1999.

LITERATURE CITED

Amijee F, Stribley DP (1987) Soluble carbohydrates of vesicular-arbuscular mycorrhizal fungi. Mycologist 21–22

Azcón-Aguilar C, Bago B (1994) Physiological characteristics of the host plant promoting an undisturbed functioning of the mycorrhizal symbiosis. *In* S Gianinazzi, H Schüepp, eds, Impact of Arbuscular Mycorrhizas on Sustainable Agriculture and Natural Ecosystems. Birkhäuser Verlag, Basel, pp 47–60

Azcón-Aguilar C, Bago B, Barea JM (1998) Saprophitic growth of AMF. *In* A Varma, B Hock, eds, Mycorrhiza: Structure, Function, Molecular Biology and Biotechnology, Ed 2. Springer-Verlag, Berlin, pp 391–408

Bago B, Azcón-Aguilar C, Goulet A, Piché Y (1998) Branched absorbing structures (BAS): a feature of the extraradical mycelium of symbiotic arbuscular mycorrhizal fungi. New Phytol **139:** 375–388

Bécard G, Doner LW, Rolin DB, Douds DD, Pfeffer PE (1991) Identification and quantification of trehalose in vesicular-arbuscular mycorrhizal fungi by *in vivo* ^{13}C NMR and HPLC analyses. New Phytol **118:** 547–552

Bécard G, Fortin A (1988) Early events of vesicular-arbuscular mycorrhiza formation on Ri T-DNA transformed roots. New Phytol **108:** 211–218

Bécard G, Piché Y (1989) Fungal growth stimulation by CO_2 and root exudates in the vesicular-arbuscular mycorrhizal symbiosis. Appl Environ Microbiol **55:** 2320–2325

Beilby JP (1983) Effects of inhibitors on early protein, RNA, and lipid synthesis in germinating vesicular-arbuscular mycorrhizal fungal spores of *Glomus caledonium.* Can J Bot **29:** 596–601

Beilby JP, Kidby DK (1980) Biochemistry of ungerminated and germinated spores of the vesicular-arbuscular mycorrhizal fungus, *Glomus caledonium*: changes in neutral and polar lipids. J Lipid Res **21:** 739–750

Bonfante P, Balestrini R, Mendgen K (1994) Storage and secretion processes in the spore of *Gigaspora margarita* Becker and Hall as revealed by high-pressure freezing and freeze substitution. New Phytol **128:** 93–101

Brosnan JT (1982) Pathways of carbon flux in gluconeogenesis. FASEB J **41:** 91–95

Bücking H, Beckmann S, Heyser W, Kottke I (1998) Elemental contents in vacuolar granules of ectomycorrhizal fungi measured by EELS and EDXS: a comparison of different methods and preparation techniques. Micron **29:** 53–61

Cox G, Sanders FE, Tinker PB, Wild JA (1975) Ultrastructural evidence relating to host- endophyte transfer in vesicular-abuscular mycorrhizas. *In* FE Sanders, B Morse, PB Tinker, eds, Endomycorrhizas. Academic Press, London, pp 297–312

Cramer CL, Davis RH (1984) Polyphosphate-cation interaction in the amino acid-containing vacuole of *Neurospora crassa*. J Biol Chem **259:** 5152–5157

Cramer CL, Vaughn LE, Davis RH (1980) Basic amino acids and inorganic polyphosphates in *Neurospora crassa*: independent regulation of vacuolar pools. J Bacteriol **142:** 945–952

Fan TW-M (1995) Recent advances in profiling plant metabolites by multi-nuclear and multidimensional NMR. *In* Y Shachar-Hill, PE Pfeffer, eds, Nuclear Magnetic Resonance in Plant Biology. American Society of Plant Physiologists, Rockville, MD, pp 181–254

Gaspar ML, Pollero RJ, Cabello MN (1994) Triacylglycerol consumption during spore germination of vesicular-arcuscular mycorrhizal fungi. J Am Oil Chem Soc **71:** 449–452

Gaspar ML, Pollero R, Cabello M (1997) Variation in lipid composition of alfalfa roots during colonization with the arbuscular mycorrhizal fungus *Glomus versiforme.* Mycologia **89:** 37–42

Gunstone FD, Pollard MR, Scrimgeour CM, Vedanayagam HS (1977) Fatty acids, part 50: ^{13}C NMR studies of olefinic fatty acids and esters. Chem Phys Lipids **18:** 115–129

Harrier LA, Wright F, Hooker JE (1998) Isolation of the 3-phosphoglycerate kinase gene of the arbuscular mycorrhizal fungus *Glomus mosseae* (Nicol.&Gerd.) Gerdemann & Trappe. Curr Genet **34:** 386–392

Harrison MJ, van Buuren ML (1995) A phosphate transporter from the mycorrhizal fungus *Glomus versiforme*. Nature **378:** 626–629

Jabaji-Hare S (1998) Lipid and fatty acid profiles of some vesicular-arbuscular mycorrhizal fungi: contribution to taxonomy. Mycologia **80:** 622–629

Jakobsen I (1995) Transport of phosphorus and carbon in VA mycorrhizas. *In* A Varma, B Hock, eds, Mycorrhiza: Structure, Function, Molecular Biology and Biotechnology. Springer-Verlag, Berlin, pp 297–323

Jennings DH (1995) The Physiology of Fungal Nutrition. Cambridge University Press, Cambridge, UK

Kulaev IS (1979) The Biochemistry of Inorganic Polyphosphates. John Wiley & Sons, Chichester, UK

London R (1988) ^{13}C-Labeling in studies of metabolic regulation. Prog NMR Spectr **20:** 337–383

Macdonald RM, Lewis M (1978) The occurrence of some acid phosphatases and dehydrogenases in the vesicular-arbuscular mycorrhizal fungus *Glomus mosseae*. New Phytol **80:** 135–141

Martin F, Marchal JP, Timinska A, Canet D (1985) The metabolism and physical state of polyphosphates in ectomycorrhizal fungi: a ^{31}P nuclear magnetic resonance study. Planta **194:** 241–246

Orlovich DA, Ashford AE (1993) Polyphosphate granules are an artifact of specimen preparation in ectomycorrhizal fungus *Pisolithus tinctorius*. Protoplasma **173:** 91–102

Pfeffer PE, Douds DD, Bécard G, Shachar-Hill Y (1999) Carbon uptake and the metabolism and transport of lipids in and arbuscular mycorrhiza. Plant Physiol **120:** 587–598

Saito M (1995) Enzyme activities of the internal hyphae and germinated spores of an arbuscular mycorrhizal fungus, *Gigaspora margarita* Becker & Hall. New Phytol **129:** 425–431

Shachar-Hill Y, Pfeffer PE, Douds D, Osman SF, Doner LW, Ratcliffe RG (1995) Partitioning of intermediate carbon metabolism in VAM colonized leek. Plant Physiol **108:** 7–15

Simon L, Bousquet J, Lévesque RC, Lalonde M (1993) Origin and diversification of endomycorrhizal fungi and coincidence with vascular land plants. Nature **363:** 67–69

Smith SE, Read DJ (1997) Mycorrhizal Symbiosis. Academic Press, London

Solaiman MD, Saito M (1997) Use of sugars by intraradical hyphae of arbuscular mycorrhizal fungi revealed by radiorespirometry. New Phytol **136:** 533–538

St-Arnaud M, Hamel C, Vimard B, Caron M, Fortin JA (1996) Enhanced hyphal growth and spore production of the arbuscular mycorrhizal fungus *Glomus intraradices* in an *in vitro* system in the absence of host roots. Mycol Res **100:** 328–332

Taylor TN, Remy W, Hass H, Kerp H (1995) Fossil arbuscular mycorrhizae from the Early Devonian. Mycologia **87:** 560–573

Thevelein JM, Hollander JA, Shulman RG (1982) Changes in the activity and properties of trehalase during early germination of yeast ascospores: correlations with trehalose breakdown as studied by *in vivo* ^{13}C NMR. Proc Natl Acad Sci USA **79:** 3503–3507